

# Modified Koufopoulos' Mechanism in the Kinetics of *in-situ* Catalytic Pyrolysis of Co-pelletized Rice Husks and Ash

Wusana Agung Wibowo<sup>1</sup>, Joko Waluyo<sup>1</sup>, Rochim Bakti Cahyono<sup>2</sup>, Rochmadi Rochmadi<sup>2</sup>, Arief Budiman<sup>2\*</sup>

<sup>1</sup> Department of Chemical Engineering, Faculty of Engineering, Universitas Sebelas Maret, Jl. Ir. Sutami 36A, 57126 Surakarta, Indonesia

<sup>2</sup> Department of Chemical Engineering, Faculty of Engineering, Universitas Gadjah Mada, Jl. Grafika 2, 55284 Yogyakarta, Indonesia

\* Corresponding author, e-mail: [abudiman@ugm.ac.id](mailto:abudiman@ugm.ac.id)

Received: 20 March 2024, Accepted: 05 July 2024, Published online: 22 August 2024

## Abstract

Using rice husk ash as a cheap *in-situ* catalyst under certain pyrolysis operating conditions can affect the yield of rice husk pyrolysis products. The two-stage semi-global kinetic models were often used to predict these yields. This research aims to study the effect of rice husk ash catalyst addition, heating rate, and pyrolysis temperature on the kinetics and yield of rice husk pellet pyrolysis products. A modified kinetic model of the Koufopoulos mechanism was proposed to predict the product's yield. The apparent pyrolysis kinetics were analyzed with the assistance of a self-designed macro-thermogravimetric analysis apparatus. The co-pelletized rice husk and ash were heated from 303 to 873 – 1173 K at 5, 10, and 40 K/min heating rates in a N<sub>2</sub> environment. Gas was collected and analyzed with gas chromatography equipped with a thermal conductivity detector at several temperature intervals during pyrolysis. It was found that the yield of the pyrolysis products can be described well by the proposed kinetic model. Adding a rice husk ash catalyst at 10 K/min reduced the activation energy of the primary gas and tar formation. It also enhanced the secondary pyrolysis reactions to form gas, which occurs more significantly at higher temperatures and heating rates. At low heating rates, heterogeneous secondary reactions tended to convert the primary tar into secondary gas. However, secondary reactions converted the primary tar into secondary tar at higher heating rates. On the other hand, increasing the pyrolysis temperature increased the gas yield and reduced the yield of tar and char.

## Keywords

rice husk ash, thermal and catalytic pyrolysis, macro-TGA, modified Koufopoulos' mechanism, products yield

## 1 Introduction

The thermal pyrolysis process has great potential to convert biomass into valuable products. Compared with thermal pyrolysis, catalytic pyrolysis can reduce the activation energy of pyrolysis by increasing the secondary reaction rate. Catalysts can convert complex reactions into semi-complex reactions with lower activation energy and produce selective pyrolysis products. Previous research has validated the effectiveness of the catalyst in biomass pyrolysis, showing its positive influence on gas yield, hydrogen concentration, and bio-oil quality while reducing tar compounds.

Rice husk ash can be a cheap alternative catalyst in biomass pyrolysis. According to Pode [1], the main content of rice husk ash is amorphous silica, which reaches 83–90%, and other contents in small amounts are alkali and alkaline earth metal compounds, including CaO, MgO, K<sub>2</sub>O,

Al<sub>2</sub>O<sub>3</sub>, Fe<sub>2</sub>O<sub>3</sub>, and Na<sub>2</sub>O. Amorphous mesoporous silica, a hydrophobic inorganic material, has high effectiveness in adsorbing and decomposing the tar content. Adding amorphous silica to catalytic tar reforming reduces the total tar [2]. On the other hand, the CaO in the catalyst fosters the pyrolysis kinetics [3].

The content of alkaline and alkaline earth metal compounds in husk ash stimulates H<sub>2</sub> formation reactions such as the Boudouard reaction, water gas-shift reaction, and hydrocarbon reformation reaction, increasing H<sub>2</sub> yield [4]. In addition, these compounds can adsorb CO<sub>2</sub>, shifting the thermodynamic conditions that help the formation of H<sub>2</sub> [5]. Rong et al. [6] studied the effect of adding a rice husk ash catalyst on tar (bio-oil) yield in rice husk pyrolysis with a 20 K/min heating rate. Adding 2% rice husk ash catalyst

resulted in a bio-oil yield of 56.07%, an increase of 4.2%, compared to no added catalyst. Meanwhile, Abu Bakar and Titiloye [7] reported rice husk catalytic pyrolysis products yield at 25 K/min with a husk ash catalyst. The gas yield increased from 18.47%wt to 21.62%wt, while the tar yield decreased from 39.61%wt to 38.29%wt.

In general, pyrolysis operating conditions, such as pyrolysis temperature, pressure, heating rate, biomass particle size, and carrier gas flow rate influence pyrolysis products' yield distribution and composition. Among these operating conditions, the influence of pyrolysis temperature and heating rate has been more widely studied. Jinn [8] studied the effect of heating rate in pyrolysis of rice husk powder on the yield and characteristics of tar. Optimum pyrolysis conditions at a heating rate of 20 K/min, feed size of 0.25–0.50 mm, pyrolysis temperature of 773 K, and N<sub>2</sub> flow rate of 100 mL/min produce a maximum liquid yield of 35.38%wt, gas yield of 28.44%wt, and char yield of 36.18%wt.

Waheed et al. [9] studied the effect of temperature and heating rate in rice husk pyrolysis on the yield and composition of gas products. Slow pyrolysis (heating rate of 10 K/min) of rice husks at a temperature of 1123 K produces a gas yield of 24.06%wt, while a gas yield of 66.61%wt is obtained in fast pyrolysis (heating rate of 300–500 K/s). Higher heating rates tend to increase gas yield [10], but according to Vieira et al. [11], raising the heating rates reduces gas yield and increases tar yield. Meanwhile, increasing the pyrolysis temperature increases gas yield [9, 12] and reduces tar yield [3].

Chemical kinetics play a vital role in explaining the characteristics of pyrolysis reactions. Most kinetic models use a lumped model approach because the kinetic model is based on the yield of lumped products, namely gas, tar, and char [13]. This pyrolysis kinetic model considers overall biomass conversion, not the conversion of biomass constituent components such as hemicellulose, cellulose, and lignin [14]. The lumped pyrolysis reaction mechanism is generally classified into one-step global, one-step multi-reaction, and two-stage semi-global models.

The global one-stage model is the simplest one that represents biomass conversion into volatile materials (tar) and char as a first-order one-stage reaction [15–17]. The kinetic parameters of one-stage global models can be estimated using isoconversional kinetic models such as the Friedmann, Kissenger, Kissenger-Akahira-Sunose (KAS), and Flynn-Wall-Ozawa (FWO) models [13, 18]. The single-step global kinetic model does not involve complex reaction mechanisms and only considers the primary pyrolysis reaction.

According to Sharma and Sheth [19], the one-stage global kinetic model fails to predict variations in pyrolysis product yield with increasing temperature.

According to Di Blasi [20], one-stage global kinetic models and one-stage multi-reaction kinetic models are unsuitable enough to simulate biomass pyrolysis reactions. Both models are simple but have the weakness of assuming a constant char and volatile yield ratio. The previous study [21] described the primary thermal degradation using the one-step reaction model, which examines a single global process. However, the one-step model does not precisely capture the weight loss (thermogravimetric, TG) data and its derivative (derivative thermogravimetry, DTG), but it can estimate the activation energy process and highlight the changes produced by the catalysts. In addition, a single-stage multi-reaction model involving the decomposition of biomass components (hemicellulose, cellulose, and lignin) precisely captured the TG data and its derivative [22]. Moreover, the developed global kinetic model proposed by Wang et al. [23] can predict hydrothermal liquefaction product yields based on chemical compositions of biomass.

Meanwhile, the two-stage semi-global kinetic model is more advantageous for simulating pyrolysis reactions because it involves primary and secondary decomposition reactions. The formation of gas from tar decomposition and the conversion of tar into char through polymerization reactions are included in the kinetic model as a secondary reaction [20, 24, 25]. This secondary reaction is considered to be in the gas/vapor phase. Koufopoulos et al. [26] proposed a pyrolysis kinetic model that assumes that gas and volatile primary pyrolysis products (tar) can react with char. These secondary reactions are thought to occur on the active surface of the char and produce different gaseous, volatile, and char products. Furthermore, developing a pyrolysis reaction model involves the formation of intermediates in the primary reaction, which are then decomposed into char [27].

The effect of direct addition of husk ash catalyst to rice husks on the yield of pyrolysis products still needs to be studied extensively. According to recent research, the *in-situ* catalytic pyrolysis process involves direct addition of the rice husk powder and ash powder in a mixed form [6]. On the other hand, the effect of direct addition of ash as a catalyst to rice husk pellets raw material on the yield of the resulting products have yet to be thoroughly studied. Improved contact between the catalyst and biomass is made possible by adding the husk ash catalyst directly to the rice husk pellets. This could change the reaction mechanism of the biomass decomposition and lead to the selective



$$Tar_1: \frac{dT_{ar_1}}{dt} = k_2 \cdot B^{n_b} - (k_4 + k_5) \cdot Tar_1^{n_r} \cdot Char_1^{n_c} \quad (5)$$

$$Char_1: \frac{dChar_1}{dt} = k_3 \cdot B^{n_b} - (k_4 + k_5) \cdot Tar_1^{n_r} \cdot Char_1^{n_c} \quad (6)$$

$$Gas_2: \frac{dGas_2}{dt} = x \cdot k_4 \cdot Tar_1^{n_r} \cdot Char_1^{n_c} \quad (7)$$

$$Tar_2: \frac{dT_{ar_2}}{dt} = y \cdot k_4 \cdot Tar_1^{n_r} \cdot Char_1^{n_c} \quad (8)$$

$$Char_2: \frac{dChar_2}{dt} = z \cdot k_5 \cdot Tar_1^{n_r} \cdot Char_1^{n_c} \quad (9)$$

$$\text{Residual: } w_{\text{model}} = B + Char_1 + Char_2 \quad (10)$$

$$\frac{dw_{\text{model}}}{dt} = \frac{dB}{dt} + \frac{dChar_1}{dt} + \frac{dChar_2}{dt} \quad (11)$$

The symbols used are explained in the Nomenclature section at the end of the paper.

In this study, the pyrolysis kinetic model for large biomass particle does not include the heat and mass transfer limitation. The reaction rate used hereinafter is the overall reaction rate, and the resulting kinetic parameter values are apparent kinetic parameters.

### 3 Numerical solution

The measured data obtained from macro-TGA experiments are then used to determine the apparent kinetic parameters using the proposed kinetic model. The objective function (OF) optimization is carried out by minimizing the sum of the squares of the differences between the experimental data and calculation results (Eq. (12)) based on the initial guess of the kinetic parameters [32, 33]:

$$\text{OF}(SSE) = \sum_{j=1}^J \left( \left( \frac{dw_{\text{exp}}}{dt} \right) - \left( \frac{dw_{\text{model}}}{dt} \right) \right)^2, \quad (12)$$

where  $J$  is the number of data points (around 1000 data). Optimization is carried out using the differential evolution (DE) method, which has the advantages of efficiency, accuracy, and reliability for optimizing highly non-linear and complex objective functions. Key control parameters in the DE algorithm include population size (NP), crossover constant (CR), and scaling factor ( $F$ ). The instructions for selecting each control parameter's value can be

found in the literature [34, 35]. The parameters  $NP = 10 \cdot N$ ,  $CR = 0.9$ , and  $F = 0.5$  were used in this study, where  $N$  is the number of kinetic parameters that fit the kinetic model.

The values of the apparent kinetic parameters ( $A_1, A_2, A_3, A_4, A_5, E_1, E_2, E_3, E_4, E_5, n_b, n_r, n_c$ ) for initial guessing refer to the results of previous research [32, 36, 37]. Meanwhile, the parameters  $x, y$ , and  $z$  are the mass conservation coefficients for the  $Gas_2, Tar_2$ , and  $Char_2$  products. The optimization step was carried out with the help of MATLAB R2021a software with the DE method optimization source code referring to Wang [38]. Furthermore, validation of the kinetic model uses two references [33], namely the coefficient of determination ( $R^2$ ) in Eq. (13) and fitness (fit(%)) in Eq. (14). In this research, the model is considered valid when the  $R^2$  value is above 0.95 and the fit(%) value is below 5%.

$$R^2 = 1 - \frac{\sum_{j=1}^J \left( \left( \frac{dw_{\text{exp}}}{dt} \right) - \left( \frac{dw_{\text{model}}}{dt} \right) \right)^2}{\sum_{j=1}^J \left( \left( \frac{dw_{\text{exp}}}{dt} \right) - \left( \frac{dw_{\text{model}}}{dt} \right)_{\text{avg}} \right)^2} \quad (13)$$

$$\text{fit}(\%) = 100 \frac{\sqrt{\text{OF}/J}}{\left( \frac{dw_{\text{exp}}}{dt} \right)_{\text{max}}} \quad (14)$$

### 4 Experimental method

#### 4.1 Co-pelletization of rice husk and ash

Rice husks in natural form and sun-dry conditions are ground using a disk mill and then sieved and classified using a standard sieve mesh. The rice husk powder used in this research was selected at 180 to 250 microns. The rice husk ash catalyst was obtained from controlled combustion of rice husk powder in a muffle furnace at 1073 K for 60 min. The ash obtained is then placed in a desiccator until ambient temperature is reached and then sieved to obtain a powder size of 180 to 250 microns. Typical analysis of rice husk and elemental and crystalline phase analysis of rice husk ash can be accessed in the previous study [17].

Before being pellet, rice husk powder and ash are mixed homogeneously with various weight ratio of rice husk to the ash of 10:0 (RRH) and 10:2 (ARH20). Next, the pellets were molded using a hydraulic press with 1 ton for 5 min without adhesive. Pellets are made in a diameter of 7 mm with a length of approximately 3–4 times the diameter.

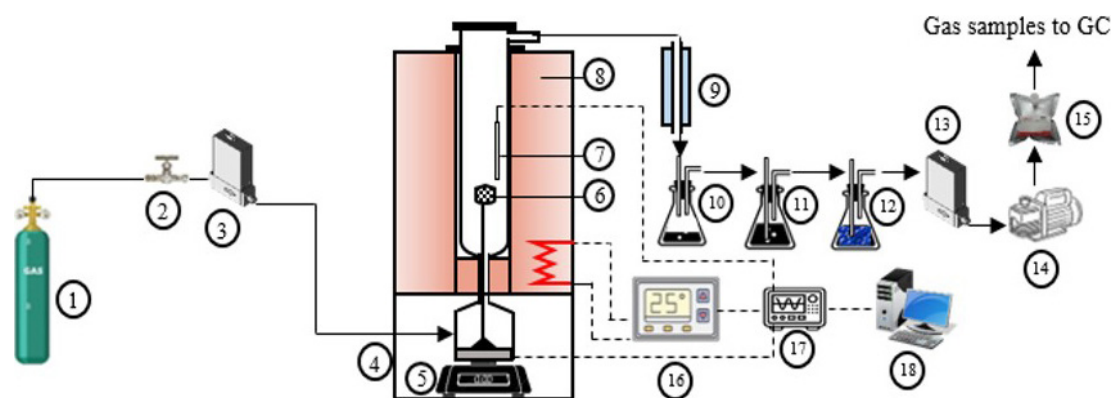


**Fig. 1** Macro-TGA apparatus; Notes: (1) N<sub>2</sub> gas cylinder; (2) Micro-valve; (3) Mass flowmeter; (4) Balance box; (5) Analytical balance; (6) Sample cup; (7) Thermocouple; (8) Furnace; (9) Condenser; (10) Condensate collector; (11) Absorber (isopropanol solvent); (12) Adsorber (silica gel); (13) Mass flowmeter; (14) Vacuum pump; (15) Gas bag; (16) Programmable thermo-controller; (17) Data logger; (18) Computer unit

#### 4.2 Macro-TGA apparatus

For the study of pyrolysis kinetics, a self-designed macro-TGA apparatus was used (see Fig. 1). The Macro-TGA consists of various components, including an electric tube furnace (8) with programmable heating rate, a stainless steel cylindrical reactor with a diameter of 8 cm and a height of 35 cm, a sample holder/support (6), and an analytical scale (5). At certain time intervals (every 1 sec), the reactor temperature was measured using a Type K thermocouple (7), and the changes in sample mass were also measured and recorded using a data logger (17), which was connected to a computer (18). Macro-TGA apparatus was designed to operate at atmospheric pressure and high temperatures. As an inert pyrolysis medium, N<sub>2</sub> gas was used, and its flow rate was regulated and measured using a digital gas mass flow meter ((2), (3)).

The gas product leaving the reactor was passed through the condenser (9), which utilizes ambient temperature water to cool and condense any condensable product. The resulting condensed product was subsequently contained in a tube (10). The non-condensed gas product was then bubbled in an absorber (11) containing iso-propanol liquid to dissolve any tar present. The gas from the absorber was then passed into a silica gel (12) to ensure the gas was not mingled with the liquid. The gas product from the silica gel was then stored in a gas bag (15) at certain temperature intervals for further analysis.

#### 4.3 Thermogravimetric analysis

In this research, thermogravimetric analysis was carried out using the assembled macro-TGA equipment. Using macro-TGA is necessary for sampling gas products resulting from pyrolysis for composition analysis and obtaining a sample mass reduction profile and reactor temperature during pyrolysis. For this purpose, a relatively large

sample of rice husk pellets is required, which is impossible using standard TGA equipment. Rice husk pellets weighing approximately 6 g were inserted into the sample holder on support and placed on an analytical balance.

Before heating begins, N<sub>2</sub> gas first flows into the reactor at a flow rate of 100 mL/min (atmospheric) for 20 min to expel the remaining oxidizing gases from the reactor. After the purging is complete, the N<sub>2</sub> flow rate is adjusted as needed, and the sample is heated with a specific heating rate (5, 10, and 40 K/min) from 303 K to the desired final pyrolysis temperature (873, 973, 1073, and 1173 K).

After reaching the final temperature, the reactor temperature is kept constant for approximately 10 min to complete the heating in the pyrolysis stage. A list of pyrolysis experiments using macro-TGA equipment is presented in Table 1. During the pyrolysis, the sample mass and reactor temperature are recorded every second using a data logger connected to a computer. The resulting gas product is stored in a gas bag for further gas composition analysis (CO, H<sub>2</sub>, CO<sub>2</sub> and CH<sub>4</sub>) using GC-TCD. Furthermore, this gas flow rate measurement is intended to calculate the mass of the pyrolysis product gas formed at specific time and temperature intervals. Meanwhile, the mass of tar condensed and absorbed in iso-propanol is calculated based on the difference between the mass of the sample consumed and the mass of gas formed.

**Table 1** Experimental setup

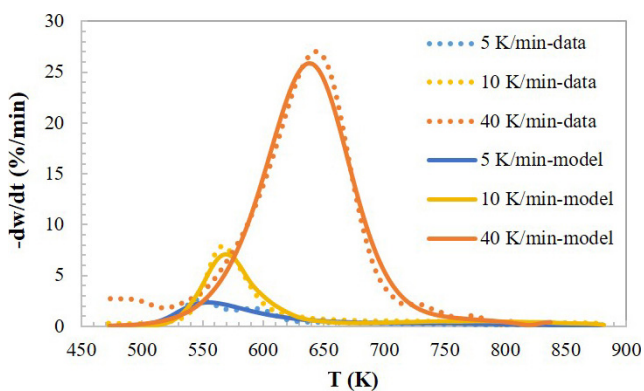
Weight ratio of RH: RHA	Sample code	Heating rate (K/min)	Pyrolysis temperature (K)
		5	873
10:0	RRH	10	873
10:2	ARH20	40	873
		40	973
10:0	RRH	40	1073
10:2	ARH20	40	1173

## 5 Results and discussion

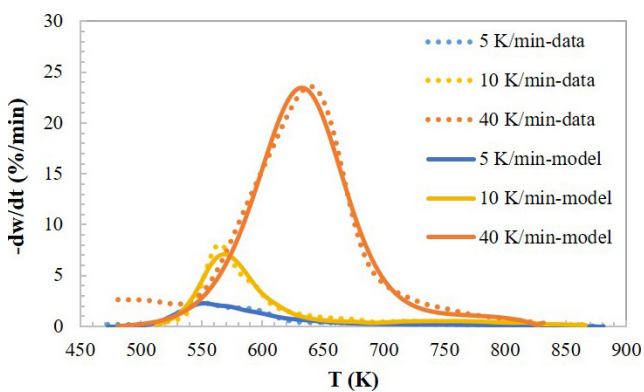
In the study of the kinetics of pyrolysis of rice husk pellets, the effect of heating rate and pyrolysis temperature was studied for non-catalytic (RRH) and catalytic (ARH20) pyrolysis.

### 5.1 Effect of heating rate

The kinetic calculations only looked at the pyrolysis zone starting at a temperature of around 500 K. The results of the mass loss rate ( $-dw/dt$  or DTG) curve fitting on non-catalytic and catalytic pyrolysis of rice husk pellets at various heating rates based on the proposed kinetic model are presented in Fig. 2. At a higher heating rate, it is found that the initial stage of pyrolysis in the DTG curve shifts towards higher temperatures, with higher and broader peaks [39]. The shift in the DTG curve is caused by increased thermal lag in the solid. A higher heating rate at the same solid temperature causes the solid to reach that temperature faster [40]. This causes a combined effect of heat and mass transfer, as well as solid decomposition kinetics at different heating rates, and is commonly found mainly in the pyrolysis of large-size particles. The effect of heating rate on the thermal characteristics of pellet pyrolysis is in line with Onsree et al. [41].



(a)



(b)

Fig. 2 Mass loss rate curve at various heating rates; (a) non-catalytic; (b) catalytic

The heating rate significantly affects the maximum mass loss rate of the solid ( $-dw/dt$  max). The higher the heating rate, the greater the maximum mass loss rate. Based on experimental data, the maximum mass loss rate was increased from 2.64%/min at 5 K/min to 7.89%/min at 10 K/min and 27.05%/min at 40 K/min for non-catalytic pyrolysis. The high heat flux at high heating rate can reduce the viscosity of the molten solid sample, thereby increasing the intensity of the volatile material formation and the mass loss rate [42]. Meanwhile, in catalytic pyrolysis, there was an increase in the maximum mass loss rate from 2.32%/min at 5 K/min to 8.05%/min at 10 K/min and 23.56%/min at 40 K/min. The maximum mass loss rate in catalytic pyrolysis tends to be slightly lower than in non-catalytic pyrolysis [43, 44]. Lower values of capacity and thermal conductivity of ash slow down the heat transfer rate of solids.

Furthermore, based on the proposed kinetic model, the yield profile of each pyrolysis product in mass fraction can be obtained, both for primary pyrolysis products ( $Gas_1$ ,  $Tar_1$  and  $Char_1$ ) and secondary pyrolysis products ( $Gas_2$ ,  $Tar_2$  and  $Char_2$ ) as a function of reaction temperature. For example, the yield profile of non-catalytic pyrolysis (RRH) and catalytic pyrolysis (ARH20) products at a heating rate of 10 K/min is presented in Fig. 3.

In the non-catalytic pyrolysis in Fig. 3 (a), it can be seen that biomass ( $B$ ) decomposes quickly, starting at a temperature of around 500 K to a temperature of around 650 K. Simultaneously with the decomposition of biomass, primary pyrolysis products begin to form in the form of primary gas ( $Gas_1$ ), primary tar ( $Tar_1$ ), and primary char ( $Char_1$ ) in parallel. Primary gas products are considered permanent gases ( $CO$ ,  $H_2$ ,  $CO_2$  and  $CH_4$ ) and are easily separated from solids.

Meanwhile, the primary tar and char products, both active, then react with each other, facilitated by the husk ash catalyst. This reaction is called a heterogeneous secondary reaction, which is thought to occur on the active surface of the char and ash catalyst, producing new gas, tar, and char compounds [26, 28]. The secondary reaction causes a decrease in the yield of the primary tar and primary char after reaching a maximum above 600 K. The secondary reaction produces products in the form of secondary gas ( $Gas_2$ ) and secondary tar ( $Tar_2$ ), as well as secondary char ( $Char_2$ ). In this research, secondary gas products are considered permanent gas with the main contents of  $CO$ ,  $H_2$ ,  $CO_2$  and  $CH_4$ . Fig. 3 (a) shows that the secondary reaction produces more  $Gas_2$  products than  $Tar_2$  and  $Char_2$ .

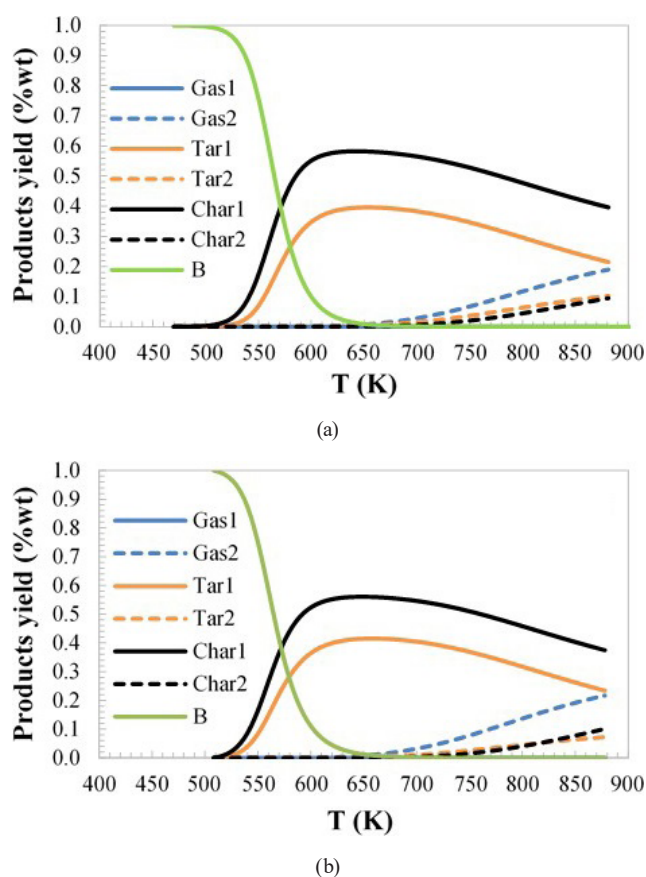


**Fig. 3** Profile of pyrolysis products at 10 K/min based on the proposed model (modified Koufopoulos' mechanism); (a) non-catalytic; (b) catalytic

Meanwhile, for ARH20 catalytic pyrolysis in Fig. 3 (b), the product yield profile obtained in catalytic pyrolysis is similar to non-catalytic pyrolysis. However, more primary tar is formed in catalytic pyrolysis than in the non-catalytic pyrolysis. Likewise, the secondary gas yield tends to be higher in catalytic pyrolysis than in non-catalytic pyrolysis. On the other hand, the yield of the secondary gas is higher than that of the secondary tar and char.

The proposed modified Koufopoulos' mechanism model can predict the yield of primary and secondary pyrolysis products at various heating rate variations, both in non-catalytic and catalytic pyrolysis. However, in practice, it is not easy to measure the yield and composition of each product quantitatively. In this research, quantitative measurements were only carried out on the mass of residual solids at various times (TG curve resulting from pyrolysis with Macro-TGA) and the permanent gas composition ( $\text{CO}$ ,  $\text{H}_2$ ,  $\text{CO}_2$ ,  $\text{CH}_4$  and  $\text{N}_2$  as carrier gas). Continuously at a specific temperature ranges, the product is stored in a gas bag with a particular volume and then analyzed using GC-TCD equipment. Examples of permanent gas composition analysis results in non-catalytic and catalytic pyrolysis of rice husk pellets with a heating rate of 10 K/min are presented in Table 2.

Based on the gas composition (%mol) in Table 2, the molar flow rate of the components (mol/min) was then calculated. The gas resulting from pyrolysis is considered an ideal gas. The flow rate of  $\text{N}_2$  as a carrier gas (100 mL/min) was considered constant throughout the pyrolysis, and the gas temperature during analysis was 303 K. Thus, the molar flow rate of  $\text{N}_2$  (mol/min) can be calculated using the ideal gas equation. Next, the molar flow rate of  $\text{H}_2$  gas is calculated by multiplying the molar flow rate of  $\text{N}_2$  by the ratio between the mole concentration of  $\text{H}_2$  and the mole concentration of  $\text{N}_2$  (%mol  $\text{H}_2$  / %mol  $\text{N}_2$ ). The same method calculates the molar flow rate of other gases ( $\text{CO}$ ,  $\text{CH}_4$  and  $\text{CO}_2$ ). Meanwhile, multiplying the component molecular weight quickly obtains the component mass flow rate (mg/min).

The time required for sampling the gas at certain temperature intervals can be calculated at a constant heating rate (for example, 10 K/min). Thus, the mass of the gas component at the average sampling temperature can

**Table 2** Gas composition (%mol) at 10 K/min

Comp.	Temperature intervals (K)						
	583–663	663–683	683–763	763–798	798–868	870–873	
Non-catalytic	$\text{H}_2$	0.05	0.04	0.03	0.30	0.56	0.65
	$\text{N}_2$	93.22	92.23	91.25	89.55	87.86	91.65
	$\text{CO}$	3.71	3.80	3.89	3.67	3.46	2.33
	$\text{CH}_4$	0.09	0.13	0.16	1.01	1.87	0.84
	$\text{CO}_2$	2.92	3.80	4.67	5.47	6.26	4.53
Catalytic	$\text{H}_2$	0.03	0.03	0.04	0.14	0.24	0.62
	$\text{N}_2$	95.08	93.60	92.12	89.64	87.16	85.06
	$\text{CO}$	2.20	2.48	2.76	3.19	3.61	3.43
	$\text{CH}_4$	0.00	0.04	0.09	0.33	0.57	0.75
	$\text{CO}_2$	2.69	3.84	5.00	6.71	8.42	10.14

be calculated as the cumulative mass fraction of permanent gas (g/g of catalyst-free sample). On the other hand, the residual solid mass fraction (solid product or char) is the catalyst-free  $w$  obtained from the mass loss data of the pyrolysis process with macro-TGA at a temperature corresponding to the average sampling temperature. Meanwhile, the cumulative mass fraction of the tar product is calculated as the difference between the initial mass fraction of the sample with the remaining mass fraction of solids and the cumulative mass fraction of gas.

On the other hand, based on the proposed kinetic model, primary pyrolysis products ( $Gas_1$ ,  $Tar_1$ ,  $Char_1$ ) and secondary pyrolysis products ( $Gas_2$ ,  $Tar_2$ ,  $Char_2$ ) were obtained. Next, the total yield of gas ( $Gas_T$ ), tar ( $Tar_T$ ), and sol-

id ( $Solid_T$ ) products can be calculated using Eqs. (15)–(17). Biomass mass fraction ( $B$ ) in Eq. (17) was added to calculate the solid product yield, intended to adjust the residual solid mass fraction data resulting from pyrolysis experiments using macro-TGA. Fig. 4 presents the total yield profile of gas, tar, and solid (char) products based on kinetic models (solid lines) and experimental data for non-catalytic and catalytic pyrolysis of rice husk pellets.

$$Gas_T = Gas_1 + Gas_2 \tag{15}$$

$$Tar_T = Tar_1 + Tar_2 \tag{16}$$

$$Solid_T = B + Char_1 + Char_2 \tag{17}$$

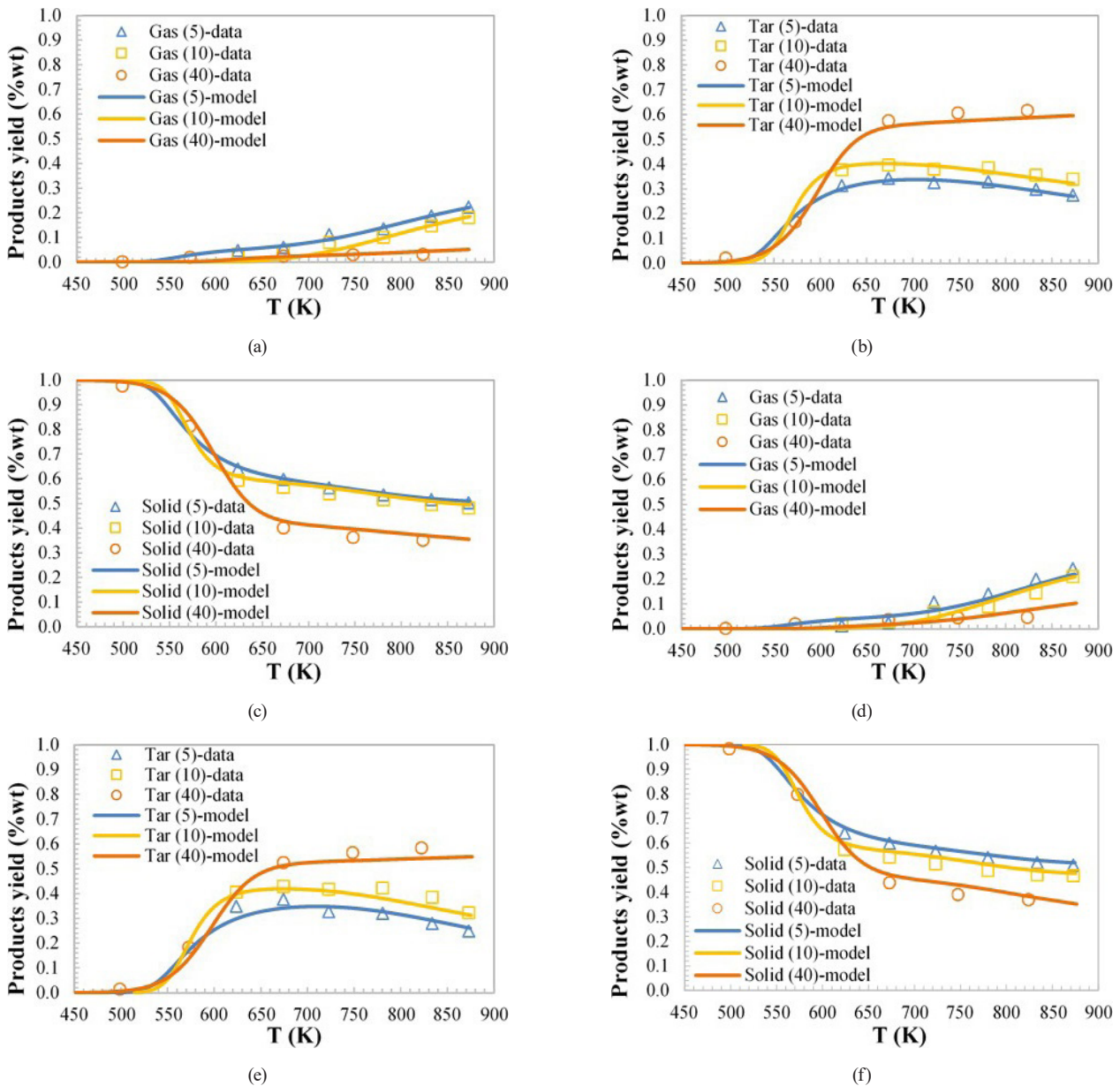


Fig. 4 Profile of rice husk pyrolysis products at varying heating rates; (a) Gas (non-catalytic); (b) Tar (non-catalytic); (c) Solid (non-catalytic); (d) Gas (catalytic); (e) Tar (catalytic); (f) Solid (catalytic)

The yield of pyrolysis products at various heating rates for non-catalytic (RRH) and catalytic (ARH20) pyrolysis of rice husk pellets, as presented in Fig. 4 (a)–(c) and Fig. 4 (d)–(f), respectively, are calculated in the mass fraction without catalyst (g/g catalyst-free sample). Fig. 4 shows that the proposed kinetic model is quite good in predicting the yield of rice husk pellet pyrolysis products. The tendency to shift the pyrolysis temperature towards higher temperatures due to increasing the heating rate [18, 45, 46] can be well represented. Based on Fig. 4, information was also obtained that increasing the heating rate tends to increase tar yield and reduce gas and char yield [11, 47, 48].

A high heating rate helps tar formation more quickly than gas formation. Meanwhile, a low heating rate causes the longer residence time of tar in the solid, which allows the cracking reaction of tar to become gas and the polymerization reaction to form char. Thus, a greater yield of gas and char is produced at a low heating rate.

Setting the heating rate to optimum conditions is usually necessary if a greater yield of a particular product is desired. In the heating rate range (5–40 K/min), pyrolysis occurs at a low heating rate if more gas product is chosen. Meanwhile, pyrolysis occurs at a high heating rate if a higher tar yield is desired.

Catalytic pyrolysis of rice husk using its ash as a catalyst tends to increase gas yield [49–51], which is more

significant at high heating rates. In addition, adding an ash catalyst tends to increase the yield of solid residue/char [46, 50, 52] and decrease the tar yield [50]. The decrease in tar yield is likely due to the high resistance to heat transfer and mass transfer in the solid with the addition of the ash catalyst. The reduction in heat transfer and mass transfer rates causes the tar from the primary pyrolysis reaction to decompose at low temperatures. This promotes the deoxygenation reactions to produce gas, alkylation, and polymerization reactions to produce more solid residue products (char and coke) [50].

The apparent kinetic parameters of non-catalytic and catalytic pyrolysis of rice husk piles at varying heating rates are presented in Table 3. Optimization of the  $Gas_2$  coefficient ( $x$ ) aims to predict the yield of gas products so that it agrees with experimental data. Meanwhile, the  $Char_2$  coefficient ( $z$ ) with a value of 2 produced the total mass fraction of all primary and secondary pyrolysis reaction products and residual biomass solids with a value of 1. Furthermore, the  $Tar_2$  ( $y$ ) coefficient is obtained from subtraction ( $z-x$ ).

In Table 3, it can be seen that  $R^2$  for all samples is in the range of 0.961–0.985, and fit(%) is in the range of 3.165%–4.873%.  $R^2$  values above 0.95 and fit(%) below 5% indicate that the proposed kinetic model can describe the non-catalytic pyrolysis reaction and catalytic pyrolysis of rice husk

**Table 3** Apparent kinetic parameters of the proposed kinetic model

Parameters	Non-catalytic			Catalytic		
	RRH-5	RRH-10	RRH-40	ARH20-5	ARH20-10	ARH20-40
SSE	0.0023	0.0011	0.0011	0.0014	0.0010	0.0011
fit(%)	4.837	3.235	3.257	3.710	3.165	3.258
$R^2$	0.961	0.978	0.985	0.980	0.979	0.984
$A_1$ (1/min)	$1.0 \cdot 10^{20}$	$7.5 \cdot 10^{18}$	$1.0 \cdot 10^{15}$	$9.9 \cdot 10^{19}$	$8.4 \cdot 10^{18}$	$1.0 \cdot 10^{15}$
$A_2$ (1/min)	$9.3 \cdot 10^{19}$	$7.0 \cdot 10^{19}$	$1.0 \cdot 10^{10}$	$9.9 \cdot 10^{19}$	$5.7 \cdot 10^{18}$	$1.0 \cdot 10^{10}$
$A_3$ (1/min)	$9.6 \cdot 10^{15}$	$1.0 \cdot 10^{16}$	$9.9 \cdot 10^{15}$	$4.6 \cdot 10^{15}$	$1.0 \cdot 10^{16}$	$4.7 \cdot 10^{15}$
$A_4$ (1/min)	$4.9 \cdot 10^4$	$1.0 \cdot 10^5$	$8.8 \cdot 10^4$	$7.1 \cdot 10^4$	$1.0 \cdot 10^5$	$1.0 \cdot 10^5$
$A_5$ (1/min)	$2.5 \cdot 10^7$	$2.9 \cdot 10^6$	$2.5 \cdot 10^7$	$3.6 \cdot 10^7$	$5.3 \cdot 10^7$	$1.1 \cdot 10^6$
$Ea_1$ (kJ/mol)	227.81	238.75	221.99	228.90	226.99	221.91
$Ea_2$ (kJ/mol)	218.91	205.55	135.07	219.11	194.09	134.74
$Ea_3$ (kJ/mol)	173.68	164.80	213.71	170.25	164.80	212.00
$Ea_4$ (kJ/mol)	70.92	70.40	80.09	75.63	70.42	78.40
$Ea_5$ (kJ/mol)	119.28	98.14	128.50	123.51	116.09	127.72
$n_b$	3.7	2.4	2.0	3.8	2.5	2.2
$n_T$	3.0	2.9	3.0	3.0	2.9	3.0
$n_C$	3.0	2.4	2.3	3.0	2.5	2.5
Coeff. $Gas_2$ ( $x$ )	1.5	1.3	0.3	1.8	1.5	0.8
Coeff. $Tar_2$ ( $y$ )	0.5	0.7	1.7	0.2	0.5	1.2
Coeff. $Char_2$ ( $z$ )	2.0	2.0	2.0	2.0	2.0	2.0

pellets at various variations in heating rate and pyrolysis temperature well. The thermogram curve in Fig. 2 also shows that the kinetic model accurately predicts solid mass loss rates.

The activation energy value for the formation of primary gas ( $Ea_1$ ) is relatively high (above 220 kJ/mol) and higher than the activation energy for the formation of primary tar ( $Ea_2$ ) and primary char ( $Ea_3$ ). Hence, the formation of primary gas is quite tricky at low temperatures. High  $Ea_1$  values were also obtained in catalytic pyrolysis; a visible decrease was obtained at 10 K/min compared to non-catalytic pyrolysis. At low heating rates (5 and 10 K/min), the activation energy of primary tar formation ( $Ea_2$ ) (205–219 kJ/mol) is higher than primary char formation ( $Ea_3$ ) (164–174 kJ/mol). Primary tar formation tends to occur more as the reaction temperature increases [53]. Meanwhile, primary char formation can occur at low temperatures. However, the opposite happens at a higher heating rate (40 K/min). The same trend was also found in catalytic pyrolysis but with slightly lower activation energy values ( $Ea_2$  and  $Ea_3$ ).

In the secondary reaction kinetics, the activation energy for the formation of secondary gas and tar ( $Ea_4$ ) (70–80 kJ/mol) is lower than the activation energy for the formation of secondary char ( $Ea_5$ ) (98–128 kJ/mol). Thus, the formation of secondary gas and tar occurs more quickly than the formation of secondary char. This tendency is also found in catalytic pyrolysis, with lower activation energy (70–78 kJ/mol), especially at high heating rates. On the other hand, the value of the secondary gas coefficient ( $x$ ) decreases with increasing heating rate, indicating that secondary tar formation tends to be higher than secondary gas formation with increasing heating rate. Meanwhile, the  $x$  value tends to be higher in catalytic pyrolysis than in non-catalytic. Thus, the addition of ash can increase the formation of secondary gases.

## 5.2 Effect of pyrolysis temperature

Based on the discussion of the influence of heating rate, information was obtained that the catalytic activity of rice husk ash began to appear at high heating rates. Under these conditions, the ash catalyst tends to encourage the

secondary reaction of tar decomposition to produce gas products in larger quantities. On the other hand, pyrolysis at high temperatures ( $\geq 973$  K) causes tar products to tend to decompose into char through a polymerization reaction [54]. Therefore, the use of the proposed kinetic model in predicting the yield of pyrolysis products at high temperatures needs to be reviewed, especially the effect of ash addition on secondary pyrolysis products.

Furthermore, the results obtained were similar in the maximum mass loss rate ( $-dw/dt$  max) at various variations in final pyrolysis temperature (see Table 4). The maximum mass loss rate in non-catalytic pyrolysis is 27.6–30.0%/min; in catalytic pyrolysis, it is obtained in the range of 28.7–30.6%/min. Meanwhile, the temperature when the maximum mass loss rate occurs ( $T_{max}$ ) is 572–590 K in non-catalytic pyrolysis and 577–586 K in catalytic pyrolysis. Table 4 shows that the kinetic model is quite good in predicting maximum mass loss velocity and  $T_{max}$ , with an absolute error below 4%.

This study obtained the maximum yield of primary tar and char, which was relatively stable (Table 5); this shows that the final pyrolysis temperature and the addition of ash did not significantly affect the primary pyrolysis reaction at high heating rates. In this study, the maximum yield of primary tar was more significant than that of primary char, indicating that tar formation at high heating rates was more dominant [48, 55, 56]. Meanwhile, the primary gas produced is much less than the primary tar and primary char products, and relatively more gas is formed at low heating rates [56].

On the other hand, increasing the pyrolysis temperature impacts changes in the yield distribution of secondary pyrolysis products, where secondary reactions generally occur at high temperatures. Based on Table 5, pyrolysis with a high final temperature increases secondary gas products significantly.

More gaseous products are formed at pyrolysis temperatures above 973 K [56]. Increasing the final pyrolysis temperature from 973 K to 1173 K causes an increase in secondary gas yield from 6.4% to 15.9% in non-catalytic pyrolysis and an increase from 8.9% to 18.5% in catalytic

**Table 4** Thermal characteristics of rice husk pellets pyrolysis at various final pyrolysis temperatures

Thermal characteristics	Type	973 K		1073 K		1173 K	
		Measured	Model	Measured	Model	Measured	Model
$-dw/dt$ max (%/min)	Non-catalytic (RRH)	27.7	27.6	27.6	28.0	30.0	29.4
	Catalytic (ARH20)	30.6	30.1	30.2	29.8	28.7	27.6
$T_{max}$ (K)	Non-catalytic (RRH)	590	587	572	568	576	573
	Catalytic (ARH20)	585	586	577	575	586	584

**Table 5** Yield of primary and secondary pyrolysis products at various final pyrolysis temperatures based on the model

Type	Final pyrolysis temperatures	Products yield at final pyrolysis temperature (%wt)						Maximum yield	
		$Gas_1$	$Tar_1$	$Char_1$	$Gas_2$	$Tar_2$	$Char_2$	$Tar_1$	$Char_1$
Non-catalytic (RRH)	973 K	0.71	26.2	10.7	6.4	30.0	25.8	55.5	36.3
	1073 K	0.22	24.4	8.3	10.2	30.6	26.3	55.8	35.3
	1173 K	0.01	19.7	4.2	15.9	29.6	30.6	54.6	34.3
Catalytic (ARH20)	973 K	1.11	20.0	5.4	8.9	35.6	29.0	54.1	36.6
	1073 K	0.00	22.3	8.6	15.4	28.6	25.1	54.6	37.1
	1173 K	0.03	23.0	4.6	18.5	27.8	26.0	57.0	34.0

pyrolysis. Even though the increase is relatively the same, secondary gas production in catalytic pyrolysis is higher than in non-catalytic pyrolysis [50]. The higher secondary gas yield in catalytic pyrolysis can be attributed to the alkali metal content in the ash having a catalytic effect on the tar decomposition reaction and promoting the formation of gas products [47].

Secondary tar decomposition reactions can occur heterogeneously on the surface of the char and catalyst and occur homogeneously within the char and catalyst pores [54, 57]. Homogeneous reactions in the gas phase can include cracking reactions, partial oxidation, condensation, and polymerization. These reactions also occur in heterogeneous tar reactions catalyzed by the active surface of char and catalyst [58]. The heterogeneous reaction between tar and char/catalyst forms additional char, CO, and CO<sub>2</sub> gas, producing many condensed tar fractions [59]. Meanwhile, homogeneous gas-phase hydrocarbon cracking generally occurs at high temperatures [60].

This study showed a significant decrease in secondary tar yield in catalytic pyrolysis with increasing final pyrolysis temperature, from 35.6%wt at 973 K to 27.8%wt at 1173 K. However, the secondary tar yield was constant at around 30%wt in non-catalytic pyrolysis. Meanwhile, the secondary char yield in catalytic pyrolysis tends to decrease with increasing final pyrolysis temperature, in contrast to non-catalytic pyrolysis. Thus, increasing the final pyrolysis temperature tends to encourage secondary gas formation reactions, which can be improved by adding a husk ash catalyst. In addition, adding an ash catalyst can inhibit additional char formation or coke formation, which increases secondary char products at high temperatures [54]. Catalytic pyrolysis at high temperatures makes the decomposition more complex, reducing char yield [57].

Increasing the pyrolysis temperature tends to increase the gas yield, while the tar yield and solid (char) yield tend to decrease. Previous researchers reported the same trend in rice husk pyrolysis [9, 61]. In this research, a significant increase in gas yield was obtained by increasing

the pyrolysis temperature from 973 K to 1173 K, namely an increase of 83% in non-catalytic pyrolysis and 86% in catalytic pyrolysis. The gas yield produced in catalytic pyrolysis is greater than that of non-catalytic pyrolysis at all pyrolysis temperatures [47, 49, 62]. The increase in gas yield is due to the secondary reaction of tar decomposition, which occurs more significantly at high temperatures and causes a decrease in the yield of tar products. This can be proven based on the yield data for non-catalytic pyrolysis products in Table 5; the primary tar fraction consumed ( $Tar_{1,max} - Tar_{1,final}$ ) (subtraction of 9<sup>th</sup> column by 4<sup>th</sup> column of Table 5) in the secondary reaction increased from 52.7% to 64% when the pyrolysis temperature increased from 973 K to 1173 K, resulting in a decrease in tar yield as well as an increase in gas yield.

On the other hand, there was a decrease in solid (char) yield of 5% in non-catalytic pyrolysis and 11% in catalytic pyrolysis with increasing pyrolysis temperature from 973 K to 1173 K. The decrease in char yield with increasing pyrolysis temperature could be caused by the primary decomposition of rice husks, which is more significant at high temperatures, or through secondary reactions of decomposition of char residues [11, 61]. The secondary reaction of char decomposition at high temperatures can also produce permanent (non-condensable) gas products, thereby increasing the yield of gas products with increasing pyrolysis temperature [62].

Based on the yield of primary and secondary pyrolysis products resulting from kinetics modeling, the yield of gas, tar, and solid (char) products is then calculated using Eqs. (15)–(17). The overall yield profile of pyrolysis products at various final pyrolysis temperatures is presented in Fig. 5. Using the proposed kinetic model is quite good in predicting the yield of rice husk pellets' non-catalytic and catalytic pyrolysis products at high temperatures. However, at temperatures above 1050 K, the proposed kinetic model cannot define the residual solids yield well (Fig. 5 (c) and Fig. 5 (f)). The decrease in the yield of residual solids (char) could be due to the partial oxidation

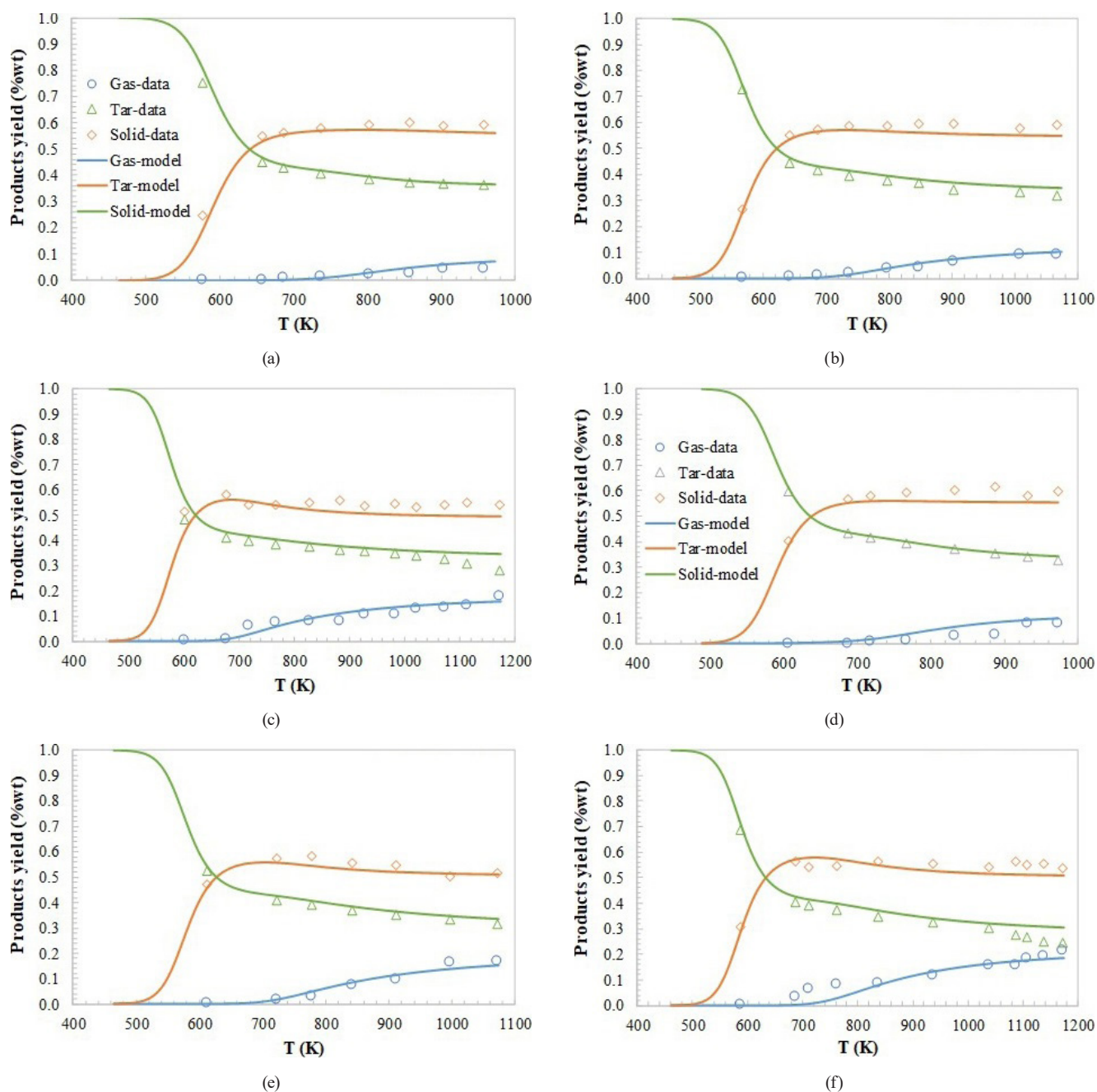


**Fig. 5** Profile of pyrolysis products at various final pyrolysis temperatures; (a) non-catalytic at 973 K; (b) non-catalytic at 1073 K; (c) non-catalytic at 1173 K; (d) catalytic at 973 K; (e) catalytic at 1073 K; (f) catalytic at 1173 K. Solid lines represent the kinetic model.

(reduction) of char by carbon dioxide ( $C + CO_2 \rightarrow 2CO$ ) which generally occurs at high temperatures [60]. The proposed kinetic model has not considered the gasification or other char decomposition reactions.

Regarding the potential for improving the quality of bio-oil products, it has been demonstrated that adding a catalyst increases the proportion of low molecular weight molecules that enhance bio-oil quality by lowering viscosity and enhancing thermal stability [63]. Adding an ash catalyst will likely strengthen the bio-oil quality by increasing its calorific value and reducing its viscosity,

density, and acid number [7, 11]. Numerous investigations have revealed that the heavy phenolic content of bio-oil can be considerably decreased by adding an ash catalyst. During pyrolysis, heavy phenolic compounds that lead to bio-oil corrosion, low heating value, high acidity, high viscosity, and instability [64] can be converted into lighter phenolic compounds or coke [65]. Meanwhile, strong Bronsted acid on the catalyst surface has been shown to improve aromatic selectivity, increasing the production of aromatic compounds [66, 67]. A higher concentration of light fraction phenolic compounds and monocyclic

aromatic hydrocarbon compounds (such as ethylbenzene and p-xylene) can increase the energy density of bio-oil and improve its miscibility with raw fossil fuels [67].

## 6 Conclusion

A modified kinetic model of the Koufopoulos mechanism provides a good description of the impact of operating parameters on the kinetics and yield of catalytic and non-catalytic rice husk pellet pyrolysis products. A higher heating rate results in higher tar production and a lower yield of gas and char. In the meantime, raising the pyrolysis temperature can result in a higher gas output and a lower yield of tar and char. Adding husk ash catalysts impacts the yield distribution of primary pyrolysis products, as primary gas forms more readily during catalytic pyrolysis. Using the husk ash catalyst promotes the secondary pyrolysis reaction to generate gas, which happens more frequently at higher pyrolysis temperatures and heating rates. This effect is more evident in the distribution of secondary pyrolysis product yields. The proposed kinetic model can be further verified by monitoring the yield of the tar product at narrow temperature intervals at more significant heating rates.

## Acknowledgment

The authors thank the Directorate General of Higher Education, Ministry of Research Technology and Higher Education, Republic of Indonesia, for their support and funding.

## References

- [1] Pode, R. "Potential application of rice husk ash waste from rice husk biomass power plant", *Renewable and Sustainable Energy Reviews*, 53, pp.1468–1485, 2016.  
<https://doi.org/10.1016/j.rser.2015.09.051>
- [2] Kobayashi, J., Kawamoto, K., Kobayashi, N. "Effect of porous silica on the removal of tar component generated from waste biomass during catalytic reforming", *Fuel Processing Technology*, 194, 106104, 2019.  
<https://doi.org/10.1016/j.fuproc.2019.05.027>
- [3] Pradana, Y. S., Daniyanto, Hartono, M., Prasakti, L., Budiman, A. "Effect of calcium and magnesium catalyst on pyrolysis kinetic of Indonesian sugarcane bagasse for biofuel production", *Energy Procedia*, 158, pp. 431–439, 2019.  
<https://doi.org/10.1016/j.egypro.2019.01.128>
- [4] Hu, S., Jiang, L., Wang, Y., Su, S., Sun, L., Xu, B., He, L., Xiang, J. "Effects of inherent alkali and alkaline earth metallic species on biomass pyrolysis at different temperatures", *Bioresource Technology*, 192, pp. 23–30, 2015.  
<https://doi.org/10.1016/j.biortech.2015.05.042>
- [5] Buentello-Montoya, D. A., Zhang, X., Li, J. "The use of gasification solid products as catalysts for tar reforming", *Renewable and Sustainable Energy Reviews*, 107, pp. 399–412, 2019.  
<https://doi.org/10.1016/j.rser.2019.03.021>
- [6] Rong, C.-X., Li, B.-X., Liu, W., Zhao, N. "The effect of oyster shell powder and rice husk ash on the pyrolysis of rice husk for bio-oil", *Energy Sources Part A: Recovery, Utilization, and Environmental Effects*, 40(11), pp. 1291–1304, 2018.  
<https://doi.org/10.1080/15567036.2018.1469690>
- [7] Abu Bakar, M. S., Titiloye, J. O. "Catalytic pyrolysis of rice husk for bio-oil production", *Journal of Analytical and Applied Pyrolysis*, 103, pp. 362–368, 2013.  
<https://doi.org/10.1016/j.jaap.2012.09.005>
- [8] Jinn, T. C. "Determination of optimum condition for the production of rice husk-derived bio-oil by slow pyrolysis process", BA Dissertation, Universiti Teknologi PETRONAS, 2013.
- [9] Waheed, Q. M. K., Nahil, M. A., Williams, P. T. "Pyrolysis of waste biomass: investigation of fast pyrolysis and slow pyrolysis process conditions on product yield and gas composition", *Journal of the Energy Institute*, 86(4), pp. 233–241, 2013.  
<https://doi.org/10.1179/1743967113Z.000000000067>
- [10] Đurić, S. N., Kaluderović, Željko L., Kosanić, T. R., Čeranić, M. B., Milotić, M. M., Brankov, S. D. "Experimental Investigation of Pyrolysis Process of Agricultural Biomass Mixture", *Periodica Polytechnica Chemical Engineering*, 58(2), pp. 141–147, 2014.  
<https://doi.org/10.3311/PPch.7199>

## Nomenclature

RRH	rice husk pellet without ash catalyst
ARH20	rice husk pellet with 20% ash catalyst
$B$	mass fraction of virgin biomass
$Gas_1$	mass fraction of primary gas
$Tar_1$	mass fraction of primary tar
$Char_1$	mass fraction of primary char
$Gas_2$	mass fraction of secondary gas
$Tar_2$	mass fraction of secondary tar
$Char_2$	mass fraction of secondary char
$Gas_T$	mass fraction of total gas
$Tar_T$	mass fraction of total tar
$Solid_T$	mass fraction of total solid (residue)
$w_{exp}$	mass fraction of solids (experiment)
$w_{model}$	mass fraction of solids (model)
$t$	time (min)
$k_i$	reaction rate constants (1/min)
$A_i$	pre-exponential factor (1/min)
$Ea_i$	activation energy (kJ/mol)
$n_B$	reaction order to $B$
$n_T$	reaction order to $Tar_1$
$n_C$	reaction order to $Char_1$
$x, y$ and $z$	coefficient for $Gas_2, Tar_2$ and $Char_2$
$R^2$	coefficient of determination
fit(%)	fitness factor
$SSE$	sum of square error
subscript $i$	reaction number 1, 2, 3, 4, 5

- [11] Vieira, F. R., Romero Luna, C. M., Arce, G. L. A. F., Ávila, I. "Optimization of slow pyrolysis process parameters using a fixed bed reactor for biochar yield from rice husk", *Biomass and Bioenergy*, 132, 105412, 2020.  
<https://doi.org/10.1016/j.biombioe.2019.105412>
- [12] Kusworo, T. D., Widayat, W., Mahadita, A. F., Firizqina, D., Utomo, D. P. "Bio-oil and Fuel Gas Production from Agricultural Waste via Pyrolysis: A Comparative Study of Oil Palm Empty Fruit Bunches (OPEFB) and Rice Husk", *Periodica Polytechnica Chemical Engineering*, 64(2), pp. 179–191, 2020.  
<https://doi.org/10.3311/PPCh.14553>
- [13] Hameed, S., Sharma, A., Pareek, V., Wu, H., Yu, Y. "A review on biomass pyrolysis models: Kinetics, network and mechanistic models", *Biomass and Bioenergy*, 123, pp. 104–122, 2019.  
<https://doi.org/10.1016/j.biombioe.2019.02.008>
- [14] Mallick, D., Buragohain, B., Mahanta, P., Moholkar, V. S. "Gasification of Mixed Biomass: Analysis Using Equilibrium, Semi-equilibrium, and Kinetic Models", In: De, S., Agarwal, A. K., Moholkar, V. S., Thallada, B. (eds.) *Coal and Biomass Gasification: Recent Advances and Future Challenges*, Springer, Singapore, 2018, pp. 223–241. ISBN 978-981-10-7334-2  
<https://doi.org/10.1007/978-981-10-7335-9>
- [15] Bilbao, R., Mastral, J. F., Ceamanos, J., Aldea, M. E. "Modelling of the pyrolysis of wet wood", *Journal of Analytical and Applied Pyrolysis*, 36(1), pp. 81–97, 1996.  
[https://doi.org/10.1016/0165-2370\(95\)00918-3](https://doi.org/10.1016/0165-2370(95)00918-3)
- [16] Jamilatun, S., Budhijanto, B., Rochmadi, R., Budiman, A. "Thermal Decomposition and Kinetic Studies of Pyrolysis of *Spirulina Platensis* Residue", *International Journal of Renewable Energy Development*, 6(3), pp. 193–201, 2017.  
<https://doi.org/10.14710/ijred.6.3.193-201>
- [17] Wibowo, W. A., Cahyono, R. B., Rochmadi, R., Budiman, A. "Thermogravimetric Analysis and Kinetic Study on Catalytic Pyrolysis of Rice Husk Pellet Using Its Ash as a Low-cost In-situ Catalyst", *International Journal of Renewable Energy Development*, 11(1), pp. 207–219, 2022.  
<https://doi.org/10.14710/ijred.2022.41887>
- [18] Widiyannita, A. M., Pradana, Y. S., Cahyono, R. B., Sutijan, Akiyama, T., Budiman, A. "Kinetic Study of Pyrolysis of Ulin Wood Residue using Thermogravimetric Analysis", *International Journal on Advanced Science, Engineering and Information Technology*, 10(4), pp. 1624–1630, 2020. [online] Available at: <http://insightso-ciety.org/ojaseit/index.php/ijaseit/article/view/3640> [Accessed: 19 March 2024]
- [19] Sharma, R., Sheth, P. N. "Multi reaction apparent kinetic scheme for the pyrolysis of large size biomass particles using macro-TGA", *Energy*, 151, pp. 1007–1017, 2018.  
<https://doi.org/10.1016/j.energy.2018.03.075>
- [20] Di Blasi, C. "Heat, momentum and mass transport through a shrinking biomass particle exposed to thermal radiation", *Chemical Engineering Science*, 51(7), pp. 1121–1132, 1996.  
[https://doi.org/10.1016/S0009-2509\(96\)80011-X](https://doi.org/10.1016/S0009-2509(96)80011-X)
- [21] Batista Jr., R., Araújo, B. S. A., Franco, P. I. B. M., Silvério, B. C., Danta, S. C., dos Santos, K. G. "Global Reaction Model to Describe the Kinetics of Catalytic Pyrolysis of Coffee Grounds Waste", *Materials Science Forum*, 899, pp 173–178, 2017.  
<https://doi.org/10.4028/www.scientific.net/MSF.899.173>
- [22] Wibowo, W. A., Cahyono, R. B., Rochmadi, R., Budiman, A. "Kinetics of In-Situ Catalytic Pyrolysis of Rice Husk Pellets Using a Multi-Component Kinetics Model", *Bulletin of Chemical Reaction Engineering & Catalysis*, 18(1), pp. 85–102, 2023.  
<https://doi.org/10.9767/bcrec.17226>
- [23] Wang, H., Han, X., Zeng, Y., Xu, C. C. "Development of a global kinetic model based on chemical compositions of lignocellulosic biomass for predicting product yields from hydrothermal liquefaction", *Renewable Energy*, 215, 118956, 2023.  
<https://doi.org/10.1016/j.renene.2023.118956>
- [24] Shafizadeh, F., Chin, P. P. S. "Thermal Deterioration of Wood", In: Goldstein, I. S. (ed.) *Wood Technology: Chemical Aspects*, American Chemical Society, 1977, pp. 57–81. ISBN 9780841203730  
<https://doi.org/10.1021/bk-1977-0043.ch005>
- [25] Antal Jr., M. J. "A Review of the Vapor Phase Pyrolysis of Biomass Derived Volatile Matter", In: Overend, R. P., Milne, T. A., Mudge, L. K. (eds.) *Fundamentals of Thermochemical Biomass Conversion*, Springer Dordrecht, 1985, pp. 511–536. ISBN 978-94-010-8685-1  
[https://doi.org/10.1007/978-94-009-4932-4\\_29](https://doi.org/10.1007/978-94-009-4932-4_29)
- [26] Koufopoulos, C. A., Papayannakos, N., Maschio, G., Lucchesi, A. "Modelling of the pyrolysis of biomass particles. Studi on kinetics, thermal and heat transfer effects", *The Canadian Journal of Chemical Engineering*, 69(4), pp. 907–915, 1991.  
<https://doi.org/10.1002/cjce.5450690413>
- [27] Park, W. C., Atreya, A., Baum, H. R. "Experimental and theoretical investigation of heat and mass transfer processes during wood pyrolysis", *Combustion and Flame*, 157(3), pp. 481–494, 2010.  
<https://doi.org/10.1016/j.combustflame.2009.10.006>
- [28] Srivastava, V. K., Sushil, Jalan, R. K. "Prediction of concentration in the pyrolysis of biomass material-II", *Energy Conversion and Management*, 37(4), pp. 473–483, 1996.  
[https://doi.org/10.1016/0196-8904\(95\)00200-6](https://doi.org/10.1016/0196-8904(95)00200-6)
- [29] Miljkovic, B., Nikolovski, B., Mitrovic, D., Janevski, J. "Modeling for Pyrolysis of Solid Biomass", *Periodica Polytechnica Chemical Engineering*, 64(2), pp. 192–204, 2020.  
<https://doi.org/10.3311/PPCh.14039>
- [30] Miljkovic, B. "Effect of Operating Parameters on Agricultural Biomass Mixture Pyrolysis Process in a Batch Reactor", *Periodica Polytechnica Chemical Engineering*, 67(1), pp. 62–73, 2023.  
<https://doi.org/10.3311/PPCh.20257>
- [31] Ramachandran, R. P. B., van Rossum, G., van Swaaij, W. P. M., Kersten, S. R. A. "Evaporation of Biomass Fast Pyrolysis Oil: Evaluation of Char Formation", *Environmental Progress & Sustainable Energy*, 28(3), pp. 410–417, 2009.  
<https://doi.org/10.1002/ep.10388>
- [32] Chen, W.-H., Eng, C. F., Lin, Y.-Y., Bach, Q.-V. "Independent parallel pyrolysis kinetics of cellulose, hemicelluloses, and lignin at various heating rates analyzed by evolutionary computation", *Energy Conversion and Management*, 221, 113165, 2020.  
<https://doi.org/10.1016/j.enconman.2020.113165>
- [33] Díez, D., Urueña, A., Piñero, R., Barrio, A., Tamminen, T. "Determination of Hemicellulose, Cellulose, and Lignin Content in Different Types of Biomasses by Thermogravimetric Analysis and Pseudocomponent Kinetic Model (TGA-PKM Method)", *Processes*, 8(9), 1048, 2020.  
<https://doi.org/10.3390/pr8091048>

- [34] Dragoi, E. N., Curteanu, S. "The use of differential evolution algorithm for solving chemical engineering problems", *Reviews in Chemical Engineering*, 32(2), pp. 149–180, 2016.  
<https://doi.org/10.1515/revce-2015-0042>
- [35] Ahmad, M. F., Isa, N. A. M., Lim, W. H., Ang, K. M. "Differential evolution: A recent review based on state-of-the-art works", *Alexandria Engineering Journal*, 61(5), pp. 3831–3872, 2022.  
<https://doi.org/10.1016/j.aej.2021.09.013>
- [36] Ragula, U. B. R., Devanathan, S., Subramanian, S. "Modeling and Optimization of Product Profiles in Biomass Pyrolysis", In: Al-Haj Ibrahim, H. (ed.) *Recent Advances in Pyrolysis*, IntechOpen, 2019, pp. 1–26. ISBN 978-1-78984-064-3  
<https://doi.org/10.5772/intechopen.85581>
- [37] Mohamed, B. A., Ellis, N., Kim, C. S., Bi, X. "Synergistic Effects of Catalyst Mixtures on Biomass Catalytic Pyrolysis", *Frontiers in Bioengineering and Biotechnology*, 8, 615134, 2020.  
<https://doi.org/10.3389/fbioe.2020.615134>
- [38] Wang, M. "Optimization Rastrigin Function by Differential Evolution algorithm. Version 1.0.0.0", [computer program] Available at: <https://www.mathworks.com/matlabcentral/fileexchange/46818-optimization-rastrigin-function-by-differential-evolution-algorithm> [Accessed: 05 March 2021]
- [39] Hu, S., Jess, A., Xu, M. "Kinetic study of Chinese biomass slow pyrolysis: Comparison of different kinetic models", *Fuel*, 86(17–18), pp. 2778–2788, 2007.  
<https://doi.org/10.1016/j.fuel.2007.02.031>
- [40] Damartzis, T., Vamvuka, D., Sfakiotakis, S., Zabaniotou, A. "Thermal degradation studies and kinetic modeling of cardoon (*Cynara cardunculus*) pyrolysis using thermogravimetric analysis (TGA)", *Bioresources Technology*, 102(10), pp. 6230–6238, 2011.  
<https://doi.org/10.1016/j.biortech.2011.02.060>
- [41] Onsree, T., Tippayawong, N., Zheng, A., Li, H. "Pyrolysis behavior and kinetics of corn residue pellets and eucalyptus wood chips in a macro thermogravimetric analyzer", *Case Studies in Thermal Engineering*, 12, pp. 546–556, 2018.  
<https://doi.org/10.1016/j.csite.2018.07.011>
- [42] Meesri, C., Moghtaderi, B. "Lack of synergetic effects in the pyrolytic characteristics of woody biomass/coal blends under low and high heating rate regimes", *Biomass and Bioenergy*, 23(1), pp. 55–66, 2002.  
[https://doi.org/10.1016/S0961-9534\(02\)00034-X](https://doi.org/10.1016/S0961-9534(02)00034-X)
- [43] Loy, A. C. M., Gan, D. K. W., Yusup, S., Chin, B. L. F., Lam, M. K., Shahbaz, M., Unrean, P., Acda, M. N., Rianawati, E. "Thermogravimetric kinetic modeling of in-situ catalytic pyrolytic conversion of rice husk to bioenergy using rice hull ash catalyst", *Bioresource Technology*, 261, pp. 213–222, 2018.  
<https://doi.org/10.1016/j.biortech.2018.04.020>
- [44] Xiang, Z., Liang, J., Morgan Jr., H. M., Liu, Y., Mao, H., Bu, Q. "Thermal behavior and kinetic study for co-pyrolysis of lignocellulosic biomass with polyethylene over Cobalt modified ZSM-5 catalyst by thermogravimetric analysis", *Bioresources Technology*, 247, pp. 804–811, 2018.  
<https://doi.org/10.1016/j.biortech.2017.09.178>
- [45] Lim, J. S., Manan, Z. A., Wan Alwi, S. R., Hashim, H. "A review on the utilisation of biomass from rice industry as a source of renewable energy", *Renewable and Sustainable Energy Reviews*, 16(5), pp. 3084–3094, 2012.  
<https://doi.org/10.1016/j.rser.2012.02.051>
- [46] Loy, A. C. M., Yusup, S., Chin, B. L. F., Gan, D. K. W., Shahbaz, M., Acda, M. N., Unrean, P., Rianawati, E. "Comparative study of in-situ catalytic pyrolysis of rice husk for syngas production: Kinetics modeling and product gas analysis", *Journal of Cleaner Production*, 197, pp. 1231–1243, 2018.  
<https://doi.org/10.1016/j.jclepro.2018.06.245>
- [47] Wang, Q., Endo, T., Apar, P., Gui, L., Chen, Q., Mitsumura, N., Qian, Q., Niida, H., Animesh, S., Sekiguchi, K. "Study On Heterogeneous Reaction Between Tar and Ash From Waste Biomass Pyrolysis And Gasification", *WIT Transactions on Ecology and the Environment*, 176, pp. 291–302, 2013.  
<https://doi.org/10.2495/ESUS130251>
- [48] Wang, Y., Kang, K., Yao, Z., Sun, G., Qiu, L., Zhao, L., Wang, G. "Effects of different heating patterns on the decomposition behavior of white pine wood during slow pyrolysis", *International Journal of Agricultural and Biological Engineering*, 11(5), pp. 218–223, 2018.  
<https://doi.org/10.25165/j.ijabe.20181105.3156>
- [49] Shen, Y., Zhao, P., Shao, Q., Takahashi, F., Yoshikawa, K. "In situ catalytic conversion of tar using rice husk char/ash supported nickel-iron catalysts for biomass pyrolytic gasification combined with the mixing-simulation in a fluidized-bed gasifier", *Applied Energy*, 160, pp. 808–819, 2015.  
<https://doi.org/10.1016/j.apenergy.2014.10.074>
- [50] Muneer, B., Zeeshan, M., Qaisar, S., Razzaq, M., Iftikhar, H. "Influence of *in-situ* and *ex-situ* HZSM-5 catalyst on co-pyrolysis of corn stalk and polystyrene with a focus on liquid yield and quality", *Journal of Cleaner Production*, 237, 117762, 2019.  
<https://doi.org/10.1016/j.jclepro.2019.117762>
- [51] Lu, Q., Zhang, T., Deng, X., He, R., Yuan, S., Li, J., Xie, X., Li, W., Liu, Z., Zhang, X. "Enhancement of gas and aromatics by in-situ catalytic pyrolysis of biomass in the presence of silica gel", *Biomass and Bioenergy*, 138, 105567, 2020.  
<https://doi.org/10.1016/j.biombioe.2020.105567>
- [52] Grafmüller, J., Böhm, A., Zhuang, Y., Spahr, S., Müller, P., Otto, T. N., Bucheli, T. D., Leifeld, J., Giger, R., Tobler, M., Schmidt, H.-P., Dahmen, N., Hagemann, N. "Wood Ash as an Additive in Biomass Pyrolysis: Effects on Biochar Yield, Properties, and Agricultural Performance", *ACS Sustainable Chemistry & Engineering*, 10(8), pp. 2720–2729, 2022.  
<https://doi.org/10.1021/acssuschemeng.1c07694>
- [53] Di Blasi, C., Branca, C. "Kinetics of Primary Product Formation from Wood Pyrolysis", *Industrial & Engineering Chemistry Research*, 40(23), pp. 5547–5556, 2001.  
<https://doi.org/10.1021/ie000997e>
- [54] Song, Y., Zhao, Y., Hu, X., Zhang, L., Sun, S., Li, C.-Z. "Destruction of tar during material volatile-char interactions at low temperature", *Fuel Processing Technology*, 171, pp. 215–222, 2018.  
<https://doi.org/10.1016/j.fuproc.2017.11.023>

- [55] Safdari, M.-S., Amini, E., Weise, D. R., Fletcher, T. H. "Heating rate and temperature effects on pyrolysis products from live wild-land fuels", *Fuel*, 242, pp. 295–304, 2019.  
<https://doi.org/10.1016/j.fuel.2019.01.040>
- [56] Kabakcı, S. B., Hacıbektaşoğlu, Ş. "Catalytic Pyrolysis of Biomass", In: Samer, M. (ed.) *Pyrolysis*, IntechOpen, 2017, pp. 167–196. ISBN 978-953-51-3312-4  
<https://doi.org/10.5772/67569>
- [57] Selvarajoo, A., Oochit, D. "Effect of pyrolysis temperature on product yields of palm fibre and its biochar characteristics", *Materials Science for Energy Technologies*, 3, pp. 575–583, 2020.  
<https://doi.org/10.1016/j.mset.2020.06.003>
- [58] Kosov, V., Kosov, V., Zaichenko, V. "Experimental Research of Heterogeneous Cracking of Pyrolysis Tars", *Chemical Engineering Transactions*, 37, pp. 211–216, 2014.  
<https://doi.org/10.3303/CET1437036>
- [59] Couhert, C., Commandre, J.-M., Salvador, S. "Is it possible to predict gas yields of any biomass after rapid pyrolysis at high temperature from its composition in cellulose, hemicellulose and lignin?", *Fuel*, 88(3), pp. 408–417, 2009.  
<https://doi.org/10.1016/j.fuel.2008.09.019>
- [60] Wang, K., Johnston, P. A., Brown, R. C. "Comparison of in-situ and ex-situ catalytic pyrolysis in a micro-reactor system", *Bioresource Technology*, 173, pp. 124–131, 2014.  
<https://doi.org/10.1016/j.biortech.2014.09.097>
- [61] Williams, P. T., Nugranad, N. "Comparison of products from the pyrolysis and catalytic pyrolysis of rice husks", *Energy*, 25(6), pp. 493–513, 2000.  
[https://doi.org/10.1016/S0360-5442\(00\)00009-8](https://doi.org/10.1016/S0360-5442(00)00009-8)
- [62] Fan, H., Chang, X., Wang, J., Zhang, Z. "Catalytic pyrolysis of agricultural and forestry wastes in a fixed-bed reactor using  $K_2CO_3$  as the catalyst", *Waste Management & Research: The Journal for a Sustainable Circular Economy*, 38(1), pp. 78–87, 2020.  
<https://doi.org/10.1177/0734242X19875508>
- [63] Kanaujia, P. K. "Production, Upgrading and Analysis of Bio-oils Derived from Lignocellulosic Biomass", In: Ramawat, K. G., Mérillon, J.-M. (eds.) *Polysaccharides*, Springer, Cham, 2014, pp. 1–26. ISBN 978-3-319-03751-6  
[https://doi.org/10.1007/978-3-319-03751-6\\_41-1](https://doi.org/10.1007/978-3-319-03751-6_41-1)
- [64] Fardhyanti, D. S., Chafidz, A., Triwibowo, B., Prsetiawan, H., Cahyani, N. N., Andriyani, S. "Improving the Quality of Bio-Oil Produced from Rice Husk Pyrolysis by Extraction of its Phenolic Compounds", *Jurnal Bahan Alam Terbarukan*, 8(2), pp. 90–100, 2019.  
<https://doi.org/10.15294/jbat.v8i2.22530>
- [65] Kim, J.-Y., Moon, J., Lee, J. H., Jin, X., Choi, J. W. "Conversion of phenol intermediates into aromatic hydrocarbons over various zeolites during lignin pyrolysis", *Fuel*, 279, 118484, 2020.  
<https://doi.org/10.1016/j.fuel.2020.118484>
- [66] Jeon, M.-J., Kim, S.-S., Jeon, J.-K., Park, S. H., Kim, J. M., Sohn, J. M., Lee, S.-H., Park, Y.-K. "Catalytic pyrolysis of waste rice husk over mesoporous materials", *Nanoscale Research Letters*, 7(1), 18, 2012.  
<https://doi.org/10.1186/1556-276X-7-18>
- [67] Arabiourrutia, M., Bensidhom, G., Bolaños, M., Trabelsi, A. B. H., Olazar, M. "Catalytic pyrolysis of date palm seeds on HZSM-5 and dolomite in a pyroprobe reactor in line with GC/MS", *Biomass Conversion and Biorefinery*, 14(2), pp. 2799–2818, 2022.  
<https://doi.org/10.1007/s13399-022-02493-2>